

# Optimization of parallel RF transmission enabled by concurrent recording of RF and gradient fields

Mustafa Cavusoglu<sup>1</sup>, Benjamin E. Dietrich<sup>1</sup>, David O. Brunner<sup>1</sup>, and Klaas P. Pruessmann<sup>1</sup>  
<sup>1</sup>Biomedical Engineering, ETH Zurich, Zurich, Zurich, Switzerland

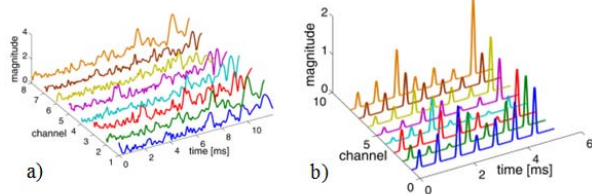


Fig. 1. Comprehensive monitoring of (a) spatially selective and (b) sparse-spokes parallel excitation pulses.

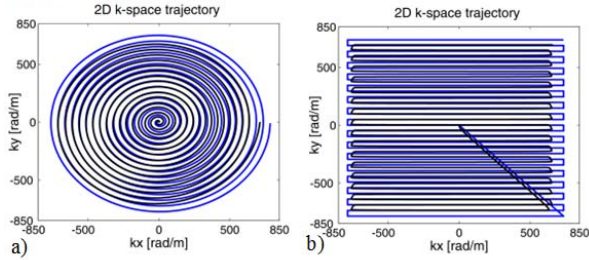


Fig. 2. Nominal (blue) and measured (black) gradient time courses for (a) spiral and (b) EPI excitations and corresponding trajectories (c) spiral (d) EPI.

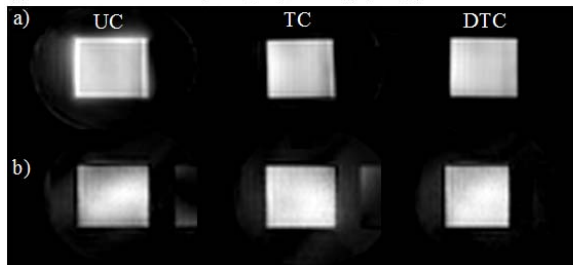


Fig. 3. Scanner results for 2 fold accelerated spatially selective (a) spiral and (b) EPI excitations for uncorrected (UC), trajectory corrected (TC) and delay plus trajectory corrected (DTC) excitations.

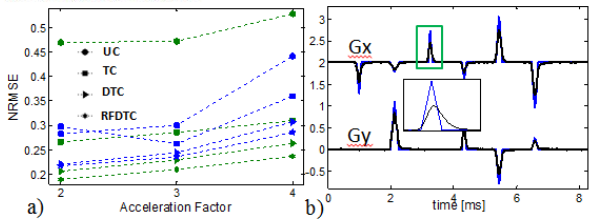


Fig. 4 (a) Normalized RMSE for accelerated excitations spiral (green) and epi (blue) (b) Nominal (blue) and measured (black) gradients for sparse-spokes pulses.

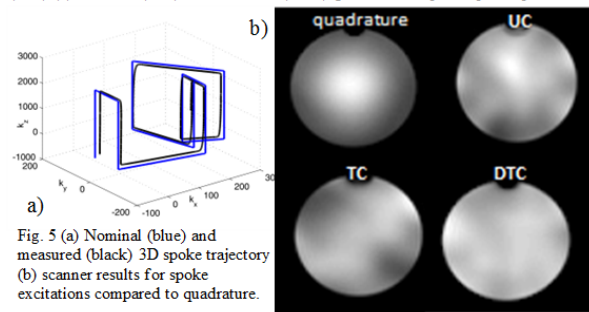


Fig. 5 (a) Nominal (blue) and measured (black) 3D spoke trajectory (b) scanner results for spoke excitations compared to quadrature.

**Introduction:** Advanced schemes of parallel excitation are based on the exact knowledge of the magnetic field dynamics inside the MR scanner and require highly accurate interplay between several RF channels and gradient waveforms. Deviations caused by various sources such as hardware imperfections, eddy currents, field drifts, externally induced fields and field fluctuations due to mechanical vibrations can therefore critically limit the accuracy of the exam (1). Further the transmit channels need to be highly synchronized and timed among themselves as well as with the gradient system especially in the case of spatially selective pulses with high acceleration factors pushing the fidelity demand. We present an optimization framework for spatially selective and sparse-spokes pulse design in parallel RF transmission at 7T based on magnetic field monitoring to measure the temporal evolution of gradient magnetic fields (to higher orders) and the multi-channel RF excitation pulses on equal time basis, fully concurrently and at full power.

**Methods: RF and gradient pulse design:** Complex valued  $B_1^+$  maps were acquired for individual channels with AFI method (2). A set of small-tip-angle parallel (8 channel) spatially selective accelerated excitation pulses  $\{b_i\}_{i=1}^{N_c}$  were designed by solving a regularized least-squares problem such as  $\arg\min_{\{b_i\}_{i=1}^{N_c}} \|\mathbf{d} - \sum_{i=1}^{N_c} \text{diag}(S_{i,j}) \mathbf{A} b_i\|_w^2 + \beta R(\mathbf{b})$  as described in ref (3) using a conjugate gradient algorithm. Spiral-in and blipped-EPI excitation pulses were designed to excite a square excitation pattern played out previous to a 3D Cartesian read-out. The trajectory was designed with a slew rate limit of 180 mT/m/s and maximum gradient strength of 25 mT/m. Target excitation pattern was sampled on a 64x64 grid with a target flip angle of 30°. Slice selective spokes pulses for  $B_1^+$  mitigation were designed using a greedy method jointly designing the RF pulse and k-space trajectory by solving  $(\mathbb{K}_N^g, \beta^g) = \arg \min_{\mathbb{K}_N \in \mathbb{R}^{2 \times 2}, \beta} \{\|\mathbf{A}(\mathbb{K}_N) \beta - \mathbf{d}\|_2^2 + \lambda \|\beta\|_2^2\}$  as described in ref (4) for 7 spokes selected from a 18x18 grid points to achieve a uniform flip angle distribution of 30°. The RF and gradient waveforms were sampled with a 6.4  $\mu$ s dwell time for scanner implementation.

**Hardware:** All measurements were performed on a Philips Achieva 7T system equipped with an 8 x 1 kW parallel transmission system (Philips Research Laboratories, Hamburg, Germany). An 8-channel loop array (Rapid Biomedical, Germany) was used for multichannel transmission with a 16-channel receive array insert (Nova Medical Inc. USA). The gradient induced field evolution has been measured using 16 <sup>19</sup>F compound based field probes (1.7 mm inner diameter) that were excited once at the beginning of the pulse to be monitored. A standalone field camera formed the basis of the applied monitoring system, comprising a 16-channel acquisition system plus the transmission and reception chains in order to operate the field sensors. The scanners' transmitters couple the RF signals into the RF lines of the sensor array where they were digitized by the same broadband converters (250 MSps with 14 bits) as the RF signals of the NMR field probes. <sup>1</sup>H and <sup>19</sup>F signal bands were separated by applying strongly band selective digital filters and down-converted to 1 MS/s in-phase/quadrature (I/Q). The RF and gradient waveforms are acquired and processed in independent data streams as shown in ref (5).

**Optimization:** Individual transmit-channels were synchronized and timed among themselves and with the gradient system by correcting for the measured delay times. For accelerated spatially selective excitations, gradient trajectory errors were minimized by redesigning the RF pulses based on the monitored gradient waveforms. RF waveform fidelity was maximized by iteratively measuring the error compensated waveforms until the deviations reach to measurement noise level. For sparse-spokes pulses, channel and spoke specific complex coefficients were updated based on the deviated spoke positions.

**Results:** Fig.1a and Fig.1b shows an example of monitoring results for multi-channel spatially selective excitation and sparse spoke pulses respectively. Fig.2a and Fig.2b shows nominal (blue) and measured (black) gradient trajectories for spiral (Fig.2c), EPI (Fig.2d) and sparse-spoke (Fig.5a) trajectories respectively. Significant deviations are seen between the nominal and measured trajectories. Fig.3a and Fig.3b shows the scanner results for 2 fold accelerated spatially selective spiral and EPI excitations. Substantial improvements in the excitations via minimizing the artifacts such as blurring, ghosting, geometrical distortions and rotations are clear and quantitatively reported in Fig.4a for trajectory corrected (TC), delay plus TC (DTC), RF waveform correction plus DTC compared to uncorrected (UC) excitations for 2-4 fold accelerations. Fig.5b shows the improvement in  $B_1^+$  mitigation for TC (std: 0.11) and DTC (std: 0.03) cases compared to UC (std: 0.17) and quadrature (std: 0.24) excitations.

**Discussion:** Parallel RF excitation pulses and gradient field evolutions were monitored with high temporal resolution and accuracy allowing a comprehensive description of the spin dynamics. Furthermore, very high precision in the temporal alignment of the RF and gradient waveforms is delivered. Improvements in spatially selective spiral pulses were majorly dominated by correcting gradient trajectory errors while EPI pulses were rather sensitive to time delay corrections. Additional phase modulations caused by the relative shifts in k-space positioning of the individual spokes as a result of relative delays in RF and gradient chains is the main contributor of the excitation error which is minimized successfully.

**References:** 1) Vannesjo et al. MRM 72, 2014 2) Yarnykh MRM 57, 2007 3) Grissom et al. MRM 56, 2006 4) Ma et al. MRM 65, 2011 5) Brunner et al. ISMRM, 2013.